haematologica
Journal of The Ferrata Storti Foundation

A novel, highly potent and selective phosphodiesterase-9 inhibitor for the treatment of sickle cell disease

by James G. McArthur, Niels Svenstrup, Chunsheng Chen, Aurelie Fricot, Caroline Carvalho, Julia Nguyen, Phong Nguyen, Anna Prachikova, Fuad Abdulla, Gregory M. Vercellotti, Olivier Hermine, Dave Edwards, Jean-Antoine Ribeil, John D. Belcher, and Thiago T. Maciel

Haematologica 2019 [Epub ahead of print]

Citation: by James G. McArthur, Niels Svenstrup, Chunsheng Chen, Aurelie Fricot, Caroline Carvalho, Julia Nguyen, Phong Nguyen, Anna Prachikova, Fuad Abdulla, Gregory M. Vercellotti, Olivier Hermine, Dave Edwards, Jean-Antoine Ribeil, John D. Belcher, and Thiago T. Maciel. A novel, highly potent and selective phosphodiesterase-9 inhibitor for the treatment of sickle cell disease.
Haematologica. 2019; 104:xxx
doi:10.3324/haematol.2018.213462

A novel, highly potent and selective phosphodiesterase-9 inhibitor for the treatment of sickle cell disease

James G. McArthur[1], Niels Svenstrup[2], Chunsheng Chen[3], Aurelie Fricot[4], Caroline Carvalho[4], Julia Nguyen[3], Phong Nguyen[3], Anna Parachikova[2], Fuad Abdulla[3], Gregory M. Vercellotti[3], Olivier Hermine[4], Dave Edwards[5], Jean-Antoine Ribeil[6], John D. Belcher[3], Thiago T. Maciel[4]

[1]Imara Inc., 700 Technology Square, 2nd Floor, Cambridge MA 02139
[2] H. Lundbeck A/S, Ottiliavej 9, 2500 Valby, Denmark
[3] Univ. Minnesota, Department of Medicine, Division of Hematology, Oncology and Transplantation, Minneapolis MN 55455 USA
[4] INSERM UMR 1163, CNRS ERL 8254; Imagine Institute, Laboratory of Excellence GR-Ex, Paris Descartes - Sorbonne Paris Cité University, Paris, France
[5] Kinexum, 8830 Glen Ferry Drive, Johns Creek GA 30022
[6] Departments of Biotherapy, Necker Children's Hospital, Assistance Publique–Hôpitaux de Paris (AP-HP), Paris Descartes - Sorbonne Paris Cité University, Paris, France

Corresponding author
James G. McArthur
700 Technology Square, 3rd Floor
Cambridge MA 02139
o: 617-231-6009
c: 617-824-0252
Email: jmcarthur@cydanco.com

KEYWORDS:

Sickle cell disease, phosphodiesterase inhibitor, PDE9, hydroxyurea

RUNNING TITLE: Novel PDE9i Therapy for Sickle Cell Disease

ABSTRACT WORD COUNT: 237

WORD COUNT: 4606

NUMBER OF FIGURES: 6

NUMBER OF TABLES: 1

Abstract

The most common treatment for patients with sickle cell disease is the chemotherapeutic, hydroxyurea, a therapy with pleiotropic effects, including increasing fetal hemoglobin in red blood cells and reducing adhesion of white blood cells to the vascular endothelium. Hydroxyurea has been proposed to mediate these effects through a mechanism of increasing cellular cGMP levels. An alternative path to increasing cGMP levels in these cells is through the use of phosphodiesterase-9 inhibitors that selectively inhibit cGMP hydrolysis and increase cellular cGMP levels. We have developed a novel, potent and selective phosphodiesterase-9 inhibitor (IMR-687) specifically for the treatment of sickle cell disease. IMR-687 increased cGMP and fetal hemoglobin in erythroid K562 and UT-7 cells and increased the percentage of fetal hemoglobin positive erythroid cells generated in vitro using a two-phase liquid culture of CD34+ progenitors from sickle cell blood or bone marrow. Oral daily dosing of IMR-687 in the Townes transgenic mouse sickle cell disease model, increased fetal hemoglobin and reduced red blood cell sickling, immune cell activation and microvascular stasis. The IMR-687 reduction in red blood cell sickling and immune cell activation was greater than seen with physiologic doses of hydroxyurea. In contrast to other described phosphodiesterase-9 inhibitors, IMR-687 did not accumulate in the central nervous system, where it would inhibit phosphodiesterase-9 in neurons, or alter rodent behavior. IMR-687 was not genotoxic or myelotoxic and did not impact fertility or fetal development in rodents. These data suggest that IMR-687 may offer a safe and effective oral alternative for hydroxyurea in the treatment of sickle cell disease.

1. Introduction

Sickle cell disease (SCD) is a genetic disease arising from a point mutation in the *HBB* gene that leads to the polymerization of hemoglobin S (HbS) during deoxygenation.[1-5] HbS forms long chains of polymers that deform RBC into a sickle shape, which impairs RBC transit in smaller blood vessels and renders them prone to hemolysis.[6,7] Increased RBC lysis and release of free HbS scavenges NO and promotes vasoconstriction, which further alters vascular biology.[8-10] This process in turn promotes the activation and mobilization of white blood cells (WBC), increasing their adhesiveness to activated endothelium.[11-16] These pathological manifestations in RBC and WBC in SCD ultimately result in the painful vaso-occlusive crises, end-organ damage and in many cases premature death.[17-19]

Hydroxyurea (HU) was the first approved disease modifying therapy for SCD.[20-24] HU was originally developed as a chemotherapeutic agent and is believed to mitigate disease pathology and organ damage sequelae by increasing RBC expression of fetal hemoglobin (HbF) and reducing WBC counts.[8,23,25-27] HU has been proposed to stimulate soluble guanyl cyclase, resulting in the elevation of cellular cGMP levels and activation of protein kinase G, which ultimately induces HbF expression.[26] HU may also indirectly affect NO biology as a result of these activities, or directly increase NO levels. Despite its activity on multiple pathways that can improve SCD pathophysiology, HU is underutilized in patients with SCD and often under-dosed.[28,29] HU utilization is challenged by responder effects and the careful safety monitoring required due to its myelosuppressive properties, and concerns about toxicities including HU impact on fertility and long-term carcinogenic potential.[30-35] As a result of these risks, female and

male patients are advised to discontinue HU therapy when trying to get pregnant or while pregnant.

The cGMP specific phosphodiesterase 9 (PDE9) enzyme degrades cGMP and therefore PDE9 inhibitors (PDE9i) increase intracellular cGMP levels recapitulating the HbF induction mechanism of HU.[36-38] PDE9 is highly expressed in erythropoietic cells, and is further elevated in neutrophils and reticulocytes from patients with SCD.[39] A PDE9i originally developed for the treatment of neurodegenerative diseases (BAY73-6691), has been shown to increase HbF transcripts in K562 cells.[38] BAY73-6691 also reduced WBC adhesion to endothelial cells, the adhesion of patient-derived neutrophils to immobilized fibronectin, leukocyte recruitment to the microvasculature, and in conjunction with HU it reduced the lethality of TNF-α induced vaso-occlusion in a mouse model of SCD.[38,40]

We describe here a novel, potent, and selective phosphodiesterase 9A inhibitor (IMR-687) that induced cGMP and HbF in the erythroid cell line K562 and increased HbF expression in erythroid cells derived from multiple SCD patients. In murine SCD models, IMR-687 increased plasma cGMP levels and HbF expression in RBC and impacted a number of disease relevant features of SCD including reducing lung inflammation, RBC sickling and occlusion of micro-vessels. Furthermore, unlike PDE9i developed for neurodegenerative diseases, IMR-687 did not alter cognition in mice and, unlike HU, did not induce myelosuppression. In summary, IMR-687 demonstrated disease-relevant improvements in several aspects of SCD with comparable efficacy to HU.

2. Methods

2.1 PDE inhibition

PDE inhibition IC50 values were determined for IMR-687 using recombinant human PDE enzymes in a radiometric assay.[41]

2.2 K562 and UT-7 erythroid cells

Human erythroleukemic K562 and UT-7 cells (American Type Culture Collection) were cultured as described in the Supplemental Methods. Terminal cell viability was determined by use of a trypan-blue exclusion technique (Thermo Fisher Scientific, France), ATP-based assays (Cell-Titer Glo, Promega) or automated cell counts (Countess Automated Cell Counter, Life Technologies). Apoptosis was assessed by Annexin V FACS assay (Biolegend).

2.3 HbF Quantification

K562 cells ($5x10^6$) supernatants were assayed using an ELISA kit for HbF (Cloud Clone Corp, CEA996Hu) (see Supplemental Methods).

Permeabolized cells were stained with PE-mouse anti-human HbF and the percentage of HbF^+ cells (% HbF) and the HbF levels (MFI) determined by flow cytometry (see Supplemental Methods).

2.5 SCD patient cells

Blood was collected from 5 severe adult SCD patients, whose ages ranged from 19 to 33 years with a median age of 32 years, admitted at the Biotherapy Department of Necker Hospital for an exchange transfusion. All samples used in this study were obtained from patients that signed informed consent forms approved by the ethical committee of Necker Hospital on 11 September 2015 (study IMNIS2015-01). $CD34^+$ cells were were cultured

in the presence of 15% BIT 9500 (mixture of bovine serum albumin [BSA] + insulin + transferrin from Stem Cell Technologies), 100 U/ml penicillin-streptomycin, 2 mM L-glutamine, 10 ng/mL recombinant human (rh) IL-3 (Peprotech), 100 ng/ml rhIL-6 (Peprotech) and 100 ng/ml rhSCF (Peprotech) for 7 days and then $CD36^+$ cells, isolated and cultured in media containing 100 ng/mL rhSCF, 10 ng/mL rhIL-3 and 2 UI/ml erythropoetin (Cilag, France) supplemented with DMSO, 30 µM HU or 10 µM IMR-687 for 5 days at which point the HbF^+ erythroid cells ($LD^-/GPA^+/Band3^+$) was determined by FACS.

2.6 Animals

2.6.1 Townes model

HbSS-Townes mice[42] on a 129/B6 background (Jackson Laboratory, Bar Harbor, ME, USA, 10-12 weeks old with 7/group) were dosed daily by gavage with vehicle (polyethylene glycol in water 1:3), 50 or 25 mg/kg of HU, or 30 mg/kg of IMR-687. On day 30 mice were anesthetized and blood counts, spleen weights, and plasma bilirubin, LDH, nitrite, HbF and free hemoglobin determined (see Supplemental Methods). Lung homogenate MPO and arginase were also determined (see Supplemental methods).

2.6.2 HbSS-Townes vaso-occlusive crisis model

HbSS-Townes mice[42] (6-17 week old with N=3/group) were treated with vehicle (0.08% w/v methyl cellulose), 100 mg/kg of HU, 10 or 30 mg/kg of IMR-687, or 100 mg/kg HU + 30 mg/kg IMR-687 in their drinking water. On day 7 of treatment, the mice were implanted with dorsal skin-fold chambers (DSFCs). Three days later, on day 10 of treatment, mice with DSFCs were anesthetized, placed on a special intravital microscopy stage, and 20-23 flowing subcutaneous venules in the DSFC window were selected and

mapped. Mice were then placed in a hypoxic atmosphere chamber (7% O_2/ 93% N_2) for one hour, after which they were returned to room air. All the selected venules were re-examined after 1 and 4 hours of re-oxygenation in room air and the number of static (no flow) venules was counted and expressed as percent stasis. After this, mice were euthanized and plasma hematocrit, bilirubin, hemoglobin and heme were measured and WBC, RBC, sickled RBC and HbF^+ RBC quantified (see Supplemental Methods).

3. Results

3.1 PDE Selectivity

To determine the selectivity of IMR-687 for the phosphodiesterase 9A, 33 recombinant human PDEs were incubated in vitro with increasing concentrations of IMR-687 and their activity determined. The IC50 of IMR-687 for PDE9A1 and PDE9A2 were 8.19 nM and 9.99 nM respectively. IMR-687 inhibited PDE9A with more than 800-fold more potency than PDE1A3, PDE1B, PDE1C, PDE5A2, with IC50 values of 88.4 µM, 8.48 µM, 12.2 µM and 81.9 µM, respectively (Table 1). Significant inhibition of the other 27 PDE enzymes tested, including PDE4 and PDE10, was not observed (Table 1).

3.2 cGMP and HbF Induction in Erythroid Cells

To determine if IMR-687 would increase cGMP levels in an erythroid cell line, actively growing K562 cells were cultured in media containing increasing concentrations of IMR-687 or HU. cGMP levels were assessed using a non-radioactive cGMP enzyme immunoassay (ENZO Life Sciences, France) with the acetylation protocol and protein

levels were quantified by the BCA assay (Pierce, France). IMR-687 incubated for 6 hours induced cGMP in a dose-dependent manner at a dose that was well tolerated (**Fig. 1A**).

Almeida and colleagues reported that exposure to the PDE9i BAY73-6691 and the sGC activator BAY 41-2271, increased HbF mRNA expression in K562 cells. To confirm this finding with IMR-687, actively growing K562 cells were exposed to increasing concentrations of IMR-687 or HU, and HbF expression was assessed by ELISA after 72 hours. IMR-687 dose-dependently induced more HbF than either BAY73-6691 or BAY 41-2271 and was 4.6 times more potent at 10 μM than a dose of HU that demonstrated cytotoxicity (**Fig. 1B**). Induction of fetal hemoglobin by IMR-687 was observed with the GM-CSF dependent erythroid line UT-7 (data not shown). While HU produced more HbF at higher concentrations, the induction was accompanied by cytotoxicity which was not observed with IMR-687 (**Fig. 1C**).

3.3 Improved SCD Phenotypes in vivo in murine model of SCD.

We next tested the impact of IMR-687 and HU on F-cells, RBC sickling and markers of hemolysis in HbSS-Townes mice. After 30 days of treatment at 30 mg/kg/day of IMR-687, we observed a greater than 3-fold increase in the percent of HbF+ F-cells (8.4% in vehicle treated and 27.3% in IMR-687 treated, $p<0.001$) (**Fig. 2A**) and a corresponding 2-fold decrease in sickled RBC (56.3% in vehicle treated and 24.4% in IMR-687 treated, $p<0.0001$) (**Fig. 2B**). We saw a similar induction of HbF and reduction in sickled RBC with mice treated with HU doses of 100 mg/kg/day (29.3% F cells and 28.8% sickled RBC). This dose which produced mortality in mice, was higher than the dose employed in patients. At HU doses that were tolerated in mice, the induction of HbF was modest and not significant compared to vehicle control (25 and 50 mg/ml/day increased F-cells

to 13% and 18% compared to 8.4% for vehicle). There was a minimal decrease in the percent sickled RBC with 25-50 mg/kg/day of HU compared to vehicle control (percent sickled RBC were decreased to 52% and 49% respectively compared to 56% for vehicle) (**Figs. 2A,B**).

The significant reduction in the RBC sickling by IMR-687 produced a corresponding decrease a reduction in markers of hemolysis. This was seen in a reduction of free plasma hemoglobin (**Fig. 2C**) where IMR-687 reduced plasma free Hg levels over 55%. HU treatment also reduced free Hg levels in a dose dependent fashion with the highest dose, 100 mg/kg, reducing levels approximately 55%.

Consistent with the reduction a reduction in hemolysis and reduction of free Hb, plasma bilirubin levels and LDH activity, markers of hemolysis[46] were significantly increased in vehicle treated SS mice compared to AA mice and reduced over 2-fold in IMR-687 treated mice (4.7 mg/dL $p<0.01$ and 102 AU $p<0.05$) (**Fig. 2D** and **2E**). The impact of the 100 mg/kg HU treatment was less pronounced, reducing bilirubin levels to 5 mg/dL ($p<0.01$) and LDH levels to 121 AU (not significant). HU dosed at 25 and 50 mg/kg did not produce a significant reduction in either marker of hemolysis.

Red cell lysis results in the release of Hb which consumes the plasma pool of NO and increases the vasculopathy associated with SCD[7] Nitrite generated in the plasma from an excess of NO produced by eNOS, can be converted back to NO as levels drop, acting as a biochemical reserve for NO.[47] In HbSS-Townes mice plasma nitrate levels are 41% lower than those in control AA mice (0.56 mg/ml versus 0.95 mg/ml) (**Fig. 2F**).

Hemolysis results in the release of hemoglobin and heme which acts as a scavenger of NO. Treatment of SS mice with 30 mg/kg of IMR-687 increased plasma nitrite levels almost 2.5-fold to 1.39 mg/ml ($p<0.05$). HU in a dose dependent manner increased nitrite levels as well, with a peak of 1.23 mg/ml in the 100 mg/kg dose group, however these changes were not significant and were modest at therapeutic doses of HU. The difference in plasma nitrite levels in IMR-687 and 100 mg/kg HU treated mice were not significantly different.

Hemolysis also results in the release of arginase which reduces NO bioavailability and is correlated with SCD mortality.[10] IMR-687 reduced lung arginase 25% ($p<0.0001$) (**Fig. 2G**) compared to vehicle controls. This effect was less pronounced in the mice treated with 100 mg/kg of HU.

Reticulocytosis reflects the bone marrow's response to anemia due to hemolysis. IMR-687 treated mice demonstrated significant changes in all measures of reticulocytosis including a 36% reduction in reticulocyte counts (**Fig. 2H**), a 27% increase in mature RBC (**Fig. 2I**), a 10% increase in hematocrit (**Fig. 2J**) and a 1.5g/dL increase in hemoglobin (**Fig. 2K**). HU at a dose of 100 mg/kg produced smaller changes in reticulocyte counts, RBC, hematocrit and hemoglobin, and the changes in hemoglobin were not significant. At HU doses of 25 and 50 mg/kg, only the change in reticulocyte counts were significant.

Townes mice have elevated circulating white blood cell counts the major component of which are neutrophils. WBC were 36% lower in IMR-687 ($24.1x10^3/mm^3$ versus $38.2x10^3/mm^3$ $p<0.05$) and 21% lower in 100mg/kg HU treatment groups ($30.4x10^3/mm^3$ versus $38.2x10^3/mm^3$) (**Fig. 3A**). While the reduction in WBC with HU

treatment can result from the myelotoxicity of HU, the IMR-687 reduction in peripheral WBC was not due to myelotoxicity as demonstrated in long-term toxicology studies conducted in normal rats (data not shown) and dogs (**Fig. 3B**) treated with IMR-687 for up to 6 and 9 months respectively. In these studies, super-physiologic doses of IMR-687 did not result in any reduction in peripheral WBC counts. Further, a histologic examination of bone marrow smears from IMR-687 treated rats and dogs did not demonstrate any myelotoxicity (data not shown). This reduction in WBC counts with IMR-687 treatment, likely reflects reduced WBC activation or mobilization in this sickle cell model.

Not only were peripheral WBC counts increased in Townes mice, but soluble WBC derived factors were elevated, including lung-associated myeloperoxidase (MPO), which is released by activated neutrophils, reduces plasma NO and contributes to vascular damage.[48] MPO levels were elevated over 5-fold in HbSS-Townes mice compared to control mice (3.1 mU/L versus 0.57 mU/L in control mice $p<0.0001$)) (**Fig**. **3C**). MPO levels were reduced 2.3-fold in IMR-687 treated mice and 2.1-fold in 100 mg/kg HU treated ice (1.3 mU/L and 1.5 mU/L respectively ($p<0.0001$)). Lower doses of HU also reduced MPO levels in the lungs.

3.4 Reduced Vaso-occlusion in HbSS-Townes Mice

Occlusion of vessels by sickled RBC and adhesive WBC in SCD leads to multi-organ pathology. To assess the impact of IMR-687 on vessel occlusion, HbSS-Townes mice were exposed to one hour of hypoxia (7% O_2/ 93% N_2) and the percentage of static venules (no blood flow) was quantified after return to normoxic conditions using a dorsal skin-fold chamber and intravital microscopy. After vehicle treated mice were returned to

normoxia, microvascular stasis was 33% and 16% after 1 (**Fig. 4A**) and 4 (**Fig. 4B**) hours, respectively. Treatment with IMR 687 for 10 days decreased stasis to 12% ($p<.01$ versus vehicle) and 7% ($p<.01$) at 30 mg/kg/day and 20% ($p<.05$) and 14% (ns) at 10 mg/kg/day after 1 and 4 hours in normoxia. Treatment of SS mice with HU at 100 mg/kg/day for 10 days decreased microvascular stasis to 13% ($p<.05$) and 8% ($p<.05$) after 1 and 4 hours. When mice were given the combination of IMR 687 (30mg/kg/day) and HU (100 mg/kg/day), stasis was 7% ($p<.01$) and 4% ($p<.01$) at 1 and 4 hours, suggesting a potential synergistic effect of the two agents.

3.5 HbF Induction in SCD Patient Erythroblasts

Erythroblasts were generated i*n vitro* using two-phase liquid culture from $CD34^+$ progenitors from 9 SCD blood or bone marrow (SCD patients undergoing hip replacement for osteonecrosis) donors. These cells were treated with IMR-687 to determine if the drug could increase HbF expression in patient-derived erythrocytes.

F-cells were determined by their expression of HbF in the LiveDead-GPA^+Band3^+ population (**Fig. 5**) by FACS. The mean for the DMSO control group (n=9) was 13.3% HbF positive. IMR-687 increased the percentage of F-cells to 21.9% ($p<0.01$, n=9). HU increased the percentage of F-cells to 22.2% ($p<0.01$, n=7, due to cytotoxicity induced by HU in 2 cultures). HU had a greater impact on the intensity of HbF staining in blood derived $CD34^+$ cells, increasing the mean fluorescence intensity (MFI) of the cells to 9744±2805 compared to 6073±1217 in control cells ($p=0.041$, n=7, due to cytotoxicity in 2 cultures), while IMR-687 increased significantly the MFI to 7813±1374 ($p<0.01$, n=9). This difference may be in part due to the greater cytotoxic stress of culturing the cells in 30 μM HU, evidenced by the loss of 2 of the 9 HU cultures.

3.6 PDE9i IMR-687 Demonstrated Low CNS Accumulation and Did Not Alter Behavior

Many PDE9i were, originally developed for neurologic diseases.[49-55] In contrast IMR-687 is a novel PDE9i selected specifically for low CNS exposure to reduce the potential impact of neuronal PDE9 inhibition on cognitive development and function. C57Bl/6J mice were dosed with IMR-687 at 10 mg/kg/day for 5 days or a CNS-active PDE9i, PF-04447943, originally developed for the treatment of neurological disorders. Plasma concentrations of the two PDE9i were very similar while the brain exposure levels of IMR-687 were 5-fold lower than those seen with PF-04447943 (**Fig. 6A**). Comparing the brain/plasma exposure profiles of the two drugs, confirmed very low concentration of IMR-687 in the CNS (7% brain/plasma ratio), compared to the PF-04447943, (41% brain/plasma ratio). Not unexpectedly, given its low brain exposure, IMR-687, showed no effect on locomotor activity or behavioral responses in toxicology studies (data not shown) nor in a classical fear conditioning mouse model of learning and memory (**Fig. 6B**) (see Supplemetnal Methods). In contrast, the brain penetrant PF-04447943 significantly increased conditioned fear responses mice at a similar dose. Beyond confirming the lack of CNS activity of IMR-687, this finding suggests that brain-penetrant PDE9i treatment could trigger cognitive modulation of unknown consequences with chronic therapy.

4. Discussion

Previous groups have described that reticulocytes and neutrophils from SCD patients express elevated levels of PDE9 and that exposure to a PDE9 inhibitor

reduced the adhesive properties and extravagation of neutrophils in sickle cell models.[38,39] They also reported the ability of this PDE9i to increase HbF mRNA levels in K562 cells. We describe a novel non-brain penetrant PDE9i, IMR-687, and its ability to increase HbF protein expression in human cell lines, patient-derived cells and mouse models of SCD and reduce many of the associated disease pathologies including reduced red cell sickling and hemolysis and normalization of white blood cell counts. Normalization of hemolysis is one of the major key improvements of SCD pathophysiology having the potential to impact "hemolytic related complications". This is the first demonstration of the reduction in hemolysis by a PDE9i. IMR-687 treatment also was efficacious in a model of vaso-occlusive crisis, preventing *in vivo* microvascular occlusion following a transient hypoxic insult. These effects were similar to the benefits seen with a high dose of HU, associated with mortality in the mouse model that was associated with some lethality in mice and cellular toxicity in vitro.

HU has been associated with activity in multiple pathways beyond cGMP, including cAMP, c-Jun kinases, epigenetic modification and regulation of miRNAs.[56] It is therefore intriguing that many of the beneficial red and white blood cell effects of HU therapy in models of SCD are recapitulated by inhibitors to a PDE9 enzyme at daily doses that were safe and well tolerated. This suggests that an optimized dose of IMR-687 may be useful as a single agent therapy for SCD. That said, IMR-687 may also have a role in combination with low dose HU in refractory patients. This may open a path for a new group of patients to see the full benefits of HU. Data in the Townes mouse model

suggested that IMR-687 and HU together had an additive effect in reducing vaso-occlusion. This effect did not seem to be mediated by an additive effect on induction of HbF or reduction in RBC sickling. It may have been through an additive effect in NO modulation, although this remains hypothetical although not unexpected given the robust reduction on hemolysis seen with IMR-687 which would reduce the release of heme, an NO scavenger. Clinically, IMR-687 is being tested in adult SCD patients both as a solo therapy and in those taking HU.

IMR-687 was purposefully developed for SCD, selected not only for potency and selectivity, but also its low brain exposure to avoid concerns about modulating cognitive function, especially in children with SCD. The data presented in this report indicate that IMR-687 has many of the beneficial *in vitro* and *in vivo* properties of HU in the context of SCD models, without the attendant toxicities of HU. Furthermore, many of the positive changes associated with HU are sufficiently recapitulated by selective targeting of the PDE9 pathway, which acts through increases in cGMP and culminates in increased HbF and ameliorates RBC pathology. This offers significant advantages over drugs that increase cGMP systemically, impacting cells that are not necessarily suitable targets, mediating side effects like hypotension. The clinical development of a safe, well-tolerated, orally available drug like IMR-687, with low CNS exposure, acting through the PDE9 pathway may offer an improved single treatment option for patients living with SCD. In light of these findings, clinical studies are underway to determine if IMR-687 might offer a safe, well-tolerated and efficacious alternative to HU therapy for SCD patients.

Acknowledgments

PDE selectivity assays were performed by SB Drug Discovery (Glasgow Scotland). We thank Dr. Michael Dussiot for his assistance on Amnis Imaging Flow Cytometer experiment and data analysis.

Authorship Contributions

TTM, AF, CC, OH were responsible for K562, UT-7, Townes and Berkeley mouse study data. CC, JN, PN, GMV, JDB were responsible for Townes mouse study data. AP, NS created IMR-687 and contributed to discussions on cell and mouse studies. TTM, AF, JAR were responsible for patient cell study data, JM led the program. JM, NS, TTM, JDB and GMV helped write and edit the manuscript.

Disclosure of Conflicts of Interest

TTM, AF, CC, OH, CC, JN, PN, GMV, JDB received financial support from Imara

NS and JM hold stock in Imara

References

1. Ingram VM. A specific chemical difference between the globins of normal human and sickle-cell anaemia haemoglobin. Nature. 1956;178(4537):792-794.
2. Bertles JF, Rabinowitz R, Dobler J. Hemoglobin interaction: modification of solid phase composition in the sickling phenomenon. Science. 1970;169(3943):375-377.
3. Ross PD, Hofrichter J, Eaton WA. Thermodynamics of gelation of sickle cell deoxyhemoglobin. J Mol Biol. 1977;115(2):111-134.
4. Platt OS, Brambilla DJ, Rosse WF, et al. Mortality in sickle cell disease. Life expectancy and risk factors for early death. N Engl J Med. 1994;330(23):1639-1644.
5. Ware RE, de Montalembert M, Tshilolo L, Abboud MR. Sickle cell disease. Lancet. 2017;390(10091):311-323.
6. Berger SA, King WS. The flow of sickle-cell blood in the capillaries. Biophys J. 1980;29(1):119-148.
7. Kato GJ, Gladwin MT, Steinberg MH. Deconstructing sickle cell disease: reappraisal of the role of hemolysis in the development of clinical subphenotypes. Blood Rev. 2007;21(1):37-47.
8. Gladwin MT, Schechter AN, Ognibene FP, et al. Divergent nitric oxide bioavailability in men and women with sickle cell disease. Circulation. 2003;107(2):271-278.
9. Reiter CD, Wang X, Tanus-Santos JE, et al. Cell-free hemoglobin limits nitric oxide bioavailability in sickle-cell disease. Nat Med. 2002;8(12):1383-1389.

10. Morris CR, Kato GJ, Poljakovic M, et al. Dysregulated arginine metabolism, hemolysis-associated pulmonary hypertension, and mortality in sickle cell disease. JAMA. 2005;294(1):81-90.

11. Belcher JD, Marker PH, Weber JP, Hebbel RP, Vercellotti GM. Activated monocytes in sickle cell disease: potential role in the activation of vascular endothelium and vaso-occlusion. Blood. 2000;96(7):2451-2459.

12. Hebbel RP, Boogaerts MA, Eaton JW, Steinberg MH. Erythrocyte adherence to endothelium in sickle-cell anemia. A possible determinant of disease severity. N Engl J Med. 1980;302(18):992-995.

13. Hebbel RP, Yamada O, Moldow CF, Jacob HS, White JG, Eaton JW. Abnormal adherence of sickle erythrocytes to cultured vascular endothelium: possible mechanism for microvascular occlusion in sickle cell disease. J Clin Invest. 1980;65(1):154-160.

14. Turhan A, Weiss LA, Mohandas N, Coller BS, Frenette PS. Primary role for adherent leukocytes in sickle cell vascular occlusion: a new paradigm. Proc Natl Acad Sci U S A. 2002;99(5):3047-3051.

15. Zennadi R, Chien A, Xu K, Batchvarova M, Telen MJ. Sickle red cells induce adhesion of lymphocytes and monocytes to endothelium. Blood. 2008;112(8):3474-3483.

16. Frenette PS. Sickle cell vaso-occlusion: multistep and multicellular paradigm. Curr Opin Hematol. 2002;9(2):101-106.

17. Nath KA, Hebbel RP. Sickle cell disease: renal manifestations and mechanisms. Nat Rev Nephrol. 2015;11(3):161-171.

18. Thornburg CD, Dixon N, Burgett S, et al. A pilot study of hydroxyurea to prevent chronic organ damage in young children with sickle cell anemia. Pediatr Blood Cancer. 2009;52(5):609-615.

19. Kassim AA, DeBaun MR. Sickle cell disease, vasculopathy, and therapeutics. Annu Rev Med. 2013;64:451-466.

20. Charache S, Terrin ML, Moore RD, et al. Effect of hydroxyurea on the frequency of painful crises in sickle cell anemia. Investigators of the Multicenter Study of Hydroxyurea in Sickle Cell Anemia. N Engl J Med. 1995;332(20):1317-1322.

21. Heeney MM, Ware RE. Hydroxyurea for children with sickle cell disease. Pediatr Clin North Am. 2008;55(2):483-501, x.

22. Maier-Redelsperger M, de Montalembert M, Flahault A, et al. Fetal hemoglobin and F-cell responses to long-term hydroxyurea treatment in young sickle cell patients. The French Study Group on Sickle Cell Disease. Blood. 1998;91(12):4472-4479.

23. Platt OS, Orkin SH, Dover G, Beardsley GP, Miller B, Nathan DG. Hydroxyurea enhances fetal hemoglobin production in sickle cell anemia. J Clin Invest. 1984;74(2):652-656.

24. Wang WC, Ware RE, Miller ST, et al. Hydroxycarbamide in very young children with sickle-cell anaemia: a multicentre, randomised, controlled trial (BABY HUG). Lancet. 2011;377(9778):1663-1672.

25. Erard F, Dean A, Schechter AN. Inhibitors of cell division reversibly modify hemoglobin concentration in human erythroleukemia K562 cells. Blood. 1981;58(6):1236-1239.

26. Cokic VP, Smith RD, Beleslin-Cokic BB, et al. Hydroxyurea induces fetal hemoglobin by the nitric oxide-dependent activation of soluble guanylyl cyclase. J Clin Invest. 2003;111(2):231-239.

27. Odievre MH, Bony V, Benkerrou M, et al. Modulation of erythroid adhesion receptor expression by hydroxyurea in children with sickle cell disease. Haematologica. 2008;93(4):502-510.

28. Stettler N, McKiernan CM, Melin CQ, Adejoro OO, Walczak NB. Proportion of adults with sickle cell anemia and pain crises receiving hydroxyurea. JAMA. 2015;313(16):1671-1672.

29. Adams-Graves P, Bronte-Jordan L. Recent treatment guidelines for managing adult patients with sickle cell disease: challenges in access to care, social issues, and adherence. Expert Rev Hematol. 2016;9(6):541-552.

30. Sheehan VA, Luo Z, Flanagan JM, et al. Genetic modifiers of sickle cell anemia in the BABY HUG cohort: influence on laboratory and clinical phenotypes. Am J Hematol. 2013;88(7):571-576.

31. Steinberg MH. Determinants of fetal hemoglobin response to hydroxyurea. Semin Hematol. 1997;34(3 Suppl 3):8-14.

32. Dover GJ, Humphries RK, Moore JG, et al. Hydroxyurea induction of hemoglobin F production in sickle cell disease: relationship between cytotoxicity and F cell production. Blood. 1986;67(3):735-738.

33. Lanzkron S, Haywood C, Jr., Hassell KL, Rand C. Provider barriers to hydroxyurea use in adults with sickle cell disease: a survey of the Sickle Cell Disease Adult Provider Network. J Natl Med Assoc. 2008;100(8):968-973.

34. Meyappan JD, Lampl M, Hsu LL. Parents' assessment of risk in sickle cell disease treatment with hydroxyurea. J Pediatr Hematol Oncol. 2005;27(12):644-650.

35. Berthaut I, Guignedoux G, Kirsch-Noir F, et al. Influence of sickle cell disease and treatment with hydroxyurea on sperm parameters and fertility of human males. Haematologica. 2008;93(7):988-993.

36. Soderling SH, Bayuga SJ, Beavo JA. Identification and characterization of a novel family of cyclic nucleotide phosphodiesterases. J Biol Chem. 1998;273(25):15553-15558.

37. Soderling SH, Bayuga SJ, Beavo JA. Cloning and characterization of a cAMP-specific cyclic nucleotide phosphodiesterase. Proc Natl Acad Sci U S A. 1998;95(15):8991-8996.

38. Almeida CB, Scheiermann C, Jang JE, et al. Hydroxyurea and a cGMP-amplifying agent have immediate benefits on acute vaso-occlusive events in sickle cell disease mice. Blood. 2012;120(14):2879-2888.

39. Almeida CB, Traina F, Lanaro C, et al. High expression of the cGMP-specific phosphodiesterase, PDE9A, in sickle cell disease (SCD) and the effects of its inhibition in erythroid cells and SCD neutrophils. Br J Haematol. 2008;142(5):836-844.

40. Miguel LI, Almeida CB, Traina F, et al. Inhibition of phosphodiesterase 9A reduces cytokine-stimulated in vitro adhesion of neutrophils from sickle cell anemia individuals. Inflamm Res. 2011;60(7):633-642.

41. Thompson WJ, Appleman MM. Multiple cyclic nucleotide phosphodiesterase activities from rat brain. Biochemistry. 1971;10(2):311-316.

42. Ryan TM, Townes TM, Reilly MP, et al. Human sickle hemoglobin in transgenic mice. Science. 1990;247(4942):566-568.

43. EC L. Peripheral Blood Smear. In: Walker HK HW, Hurst JW, ed. Clinical Methods: The History, Physical, and Laboratory Examinations. Boston: Butterworths; 1990.

44. Kleihauer E, Braun H, Betke K. [Demonstration of fetal hemoglobin in erythrocytes of a blood smear]. Klin Wochenschr. 1957;35(12):637-638.

45. Fairbanks VF, Ziesmer SC, O'Brien PC. Methods for measuring plasma hemoglobin in micromolar concentration compared. Clin Chem. 1992;38(1):132-140.

46. Kato GJ, McGowan V, Machado RF, et al. Lactate dehydrogenase as a biomarker of hemolysis-associated nitric oxide resistance, priapism, leg ulceration, pulmonary hypertension, and death in patients with sickle cell disease. Blood. 2006;107(6):2279-2285.

47. Dezfulian C, Raat N, Shiva S, Gladwin MT. Role of the anion nitrite in ischemia-reperfusion cytoprotection and therapeutics. Cardiovasc Res. 2007;75(2):327-338.

48. Zhang H, Xu H, Weihrauch D, et al. Inhibition of myeloperoxidase decreases vascular oxidative stress and increases vasodilatation in sickle cell disease mice. J Lipid Res. 2013;54(11):3009-3015.

49. da Silva FH, Pereira MN, Franco-Penteado CF, De Nucci G, Antunes E, Claudino MA. Phosphodiesterase-9 (PDE9) inhibition with BAY 73-6691 increases corpus

cavernosum relaxations mediated by nitric oxide-cyclic GMP pathway in mice. Int J Impot Res. 2013;25(2):69-73.

50. Hutson PH, Finger EN, Magliaro BC, et al. The selective phosphodiesterase 9 (PDE9) inhibitor PF-04447943 (6-[(3S,4S)-4-methyl-1-(pyrimidin-2-ylmethyl)pyrrolidin-3-yl]-1-(tetrahydro-2H-py ran-4-yl)-1,5-dihydro-4H-pyrazolo[3,4-d]pyrimidin-4-one) enhances synaptic plasticity and cognitive function in rodents. Neuropharmacology. 2011;61(4):665-676.

51. Vardigan JD, Converso A, Hutson PH, Uslaner JM. The selective phosphodiesterase 9 (PDE9) inhibitor PF-04447943 attenuates a scopolamine-induced deficit in a novel rodent attention task. J Neurogenet. 2011;25(4):120-126.

52. van der Staay FJ, Rutten K, Barfacker L, et al. The novel selective PDE9 inhibitor BAY 73-6691 improves learning and memory in rodents. Neuropharmacology. 2008;55(5):908-918.

53. Prickaerts J, Heckman PRA, Blokland A. Investigational phosphodiesterase inhibitors in phase I and phase II clinical trials for Alzheimer's disease. Expert Opin Investig Drugs. 2017;26(9):1033-1048.

54. Heckman PR, Wouters C, Prickaerts J. Phosphodiesterase inhibitors as a target for cognition enhancement in aging and Alzheimer's disease: a translational overview. Curr Pharm Des. 2015;21(3):317-331.

55. Saavedra A, Giralt A, Arumi H, Alberch J, Perez-Navarro E. Regulation of hippocampal cGMP levels as a candidate to treat cognitive deficits in Huntington's disease. PLoS One. 2013;8(9):e73664.

56. Pule GD, Mowla S, Novitzky N, Wiysonge CS, Wonkam A. A systematic review of known mechanisms of hydroxyurea-induced fetal hemoglobin for treatment of sickle cell disease. Expert Rev Hematol. 2015;8(5):669-679.

Table 1. Phosphodiesterase (PDE) Selectivity of IMR-687. Enzyme inhibition by IMR-687 on human recombinant PDEs demonstrated was selective to PDE9 by 1000-10000 fold over PDE1A3, 1B, 1C, and PDE5A2 isoforms. No measurable inhibition was observed in PDE2A3, 3A, 3B, 4A1, 4A4, 4A10, 4B1, 4B2, 4B3, 4C2, 4D1, 4D2, 4D3, 4D4, 4D5, 4D7, 5A1, 5A3, 6AB, 6C, 7A, 7B, 8A1, 8B, 10A1, 10A2 or 11A1 at doses up to 100uM.

NI= No inhibition detected

Enzyme	**IC_{50} (μM)**	**Enzyme**	**IC_{50} (μM)**
PDE1A3	88.4	PDE4D4	NI
PDE1B	8.48	PDE4D5	NI
PDE1C	12.2	PDE4D7	NI
PDE2A3	NI	PDE5A1	>100
PDE3A	NI	PDE5A2	81.9
PDE3B	NI	PDE5A3	>100
PDE4A1	>100	PDE6AB	NI
PDE4A4	>100	PDE6C	NI
PDEA10	NI	PDE7A	NI
PDE4B1	NI	PDE7B	>100
PDE4B2	>100	PDE8A1	NI
PDE4B3	>100	PDE8B	NI
PDE4C2	NI	**PDE9A1**	**0.008**
PDE4D1	>100	**PDE9A2**	**0.010**
PDE4D2	>100	PDE10A2	>100
PDE4D3	NI	PDE11A1	NI

Figure Legends

Figure 1. IMR-687 recapitulates the cGMP and fetal hemoglobin (HbF) induction mechanism of hydroxyurea (HU) in erythroid cells. (A) IMR-687 and HU treatment for 6 hours in erythroid K562 cells increases cGMP in a dose-dependent manner. **(B)** IMR-687 and HU treatment in erythroid K562 cells for 72 hours also induced HbF in a dose-dependent manner, evaluated by an ELISA assay using an antibody against human fetal hemoglobin. **(C)** HU demonstrates greater cytotoxicity than IMR-687 as assessed by cell counts at the end of a 72 hour culture with wach drug. *$p<0.05$, **$p<0.01$, ***$p<0.001$. Data presented are means ± standard errors.

Figure 2. Treatment of IMR-687 in sickle mice for 30 days results in fetal hemoglobin (HbF) induction, reduced hemolysis and reduced reticulocytosis. Townes-HBSS mice were dosed orally for 30 days with IMR-687 at 30 mg/kg or HU at 25, 50 or 100 mg/kg. Treatment with IMR-687, or HU at the highest dose, resulted in an increase in of fetal hemoglobin **(A)** in Ter-119^+ red blood cells, reduction in the percentage of RBC with a sickle shape observed on blood smear **(B)** and a reduction in hemolysis as indicated by reduced plasma free hemoglobin **(C)**, plasma bilirubin **(D)** and lactate dehydrogenase (LDH) **(E)** levels and indirectly with an increase in plasma nitrate levels **(F)** and reduction in lung arginase levels **(G)**. Commensurate with these changes there was a reduction in evidence in reticulocytosis including reduced reticulocyte counts **(H)**, increased mature red blood cell (RBC) counts **(I)**, increased hematocrit **(J)** and hemoglobin **(K)**. Statistical significance was calculated for each agent and dose compared to a vehicle-treated control (N=7). *$p<0.05$; **$p<0.01$; ***$p<0.001$. NS = not significant ($p>0.05$). Data presented are means ± standard errors.

Figure 3. Treatment of IMR-687 in sickle mice for 30 days results in reduced immune cell activity. White blood cell **(**WBC) counts are elevated in Townes mice above normal controls **(A)**. Townes-HBSS mice were dosed orally for 30 days with IMR-687 at 30 mg/kg or HU at 100 mg/kg. Treatment with IMR-687 or HU reduced circulating WBC counts **(A)**. (N=3). NS = not significant, *$p>0.05$. Data presented are means ± standard errors. This decrease in WBC counts is not seen in normal mice, rats or dogs dosed with IMR-687 including long term 9 month toxicology studies in dogs dosed orally daily with 10, 25 or 50 mg/kg of IMR-687 **(B)**. Along with the reduction in circulating WBC levels in IMR-687 treated Townes mice, there was a significant reduction in lung myeloperoxidase activity **(C)**. (N=7). **$p<0.01$; ***$p<0.001$. NS = not significant ($p>0.05$). Data presented are means ± standard errors.

Figure 4. Treatment with IMR-687 reduces vessel-occlusion in the Townes-HbSS sickle cell disease model. Townes-HBSS mice were dosed orally for 30 days with IMR-687 at 30 or 10 mg/kg or HU at 100 mg/kg or 30 mg/kg IMR-687 in combination with 100 mg/kg HU. After 10 days of treatment, animals were exposed to hypoxic conditions for quantification of microvessel occlusion via dorsal skin-fold chambers implanted on Day 7 of treatment. On day 10 of treatment, 20-23 flowing venules in the chamber window were selected and mapped. Mice were then exposed to 1h of hypoxia (7% O_2) and then returned to room air. The same venules were re-examined at 1h **(A)** and 4h **(B)** post hypoxia for blood flow and static (no flow) venules were counted and the data expressed as percent stasis. Data presented are means ± standard deviations. Statistical significance was calculated for each agent and dose compared to a vehicle-treated control. *, $p<0.05$; **, $p<0.01$; NS = not significant ($p>0.05$). Data presented are means ± standard errors.

Figure 5. IMR-687 increases F-cells in patient-derived sickle cell disease (SCD) $CD36^+$ cells. CD36+ cells derived from CD34+ adult SCD peripheral blood cells were cultured as described in Methods. The increase in the percentage of F-cells for each treatment is depicted. Statistical significance was calculated for each agent compared to a vehicle-treated control (N=9). **$p<0.01$; ; NS = not significant ($p>0.05$). Errors presented as standard error.

Figure 6. A brain-penetrant phosphodiesterase-9 inhibitor (PDE9i) but not IMR-687 increases fear responses in a model of learning and memory. (A) Fear conditioning responses are increased and persistent in mice treated with a brain-penetrant PDE9i compared to vehicle-treated or IMR-687-treated mice. **(B)** Drug exposure of the brain-penetrant PDE9i is five-fold greater than that of IMR-687. Errors presented as standard error.

1A

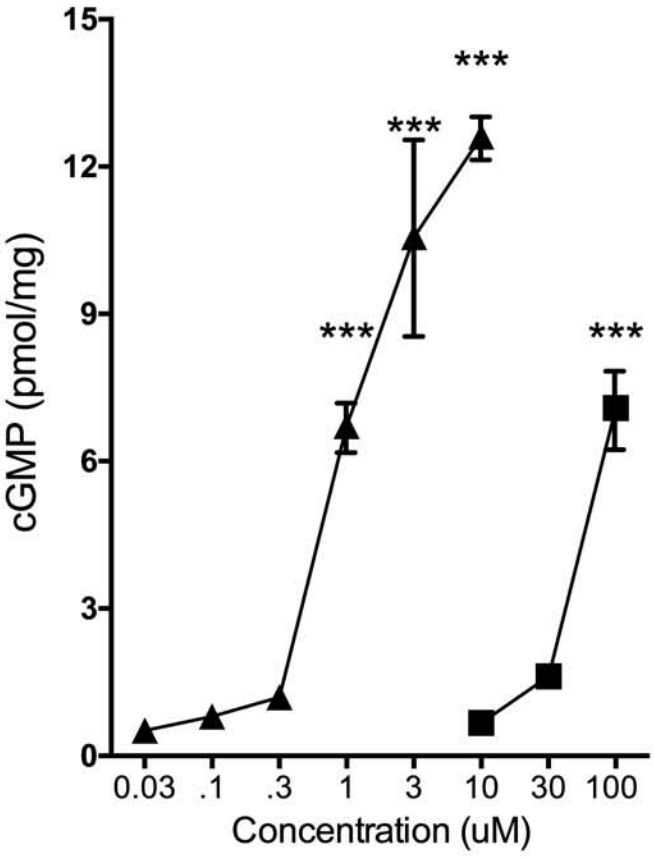
15
12
9
6
3
0
cGMP (pmol/mg)
***
***
***
***
0.03
.1
.3
1
3
10
30
100
Concentration (uM)

1B

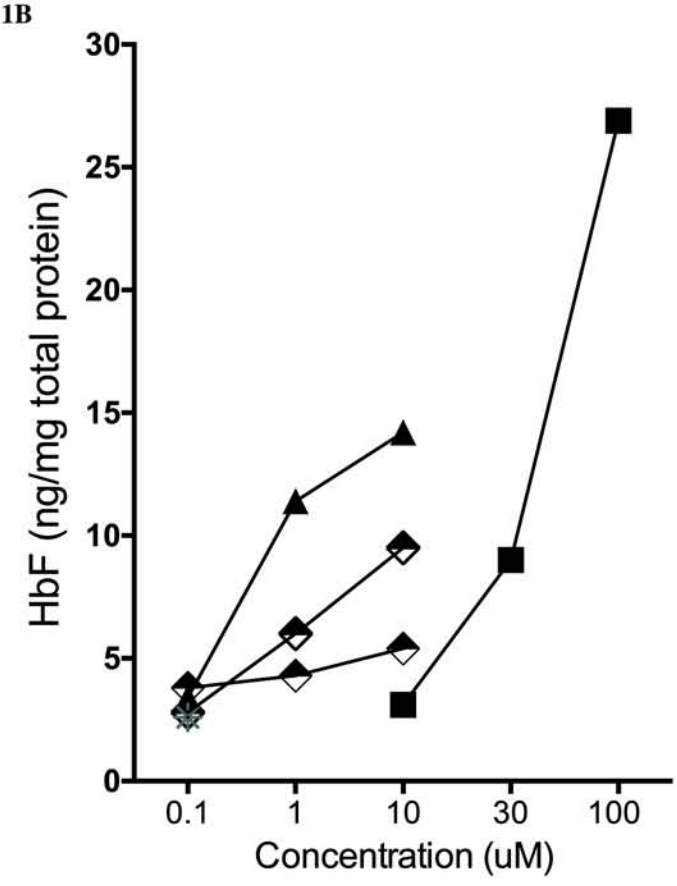
30
25
20
15
10
5
0
HbF (ng/mg total protein)
0.1
1
10
30
100
Concentration (uM)

1C

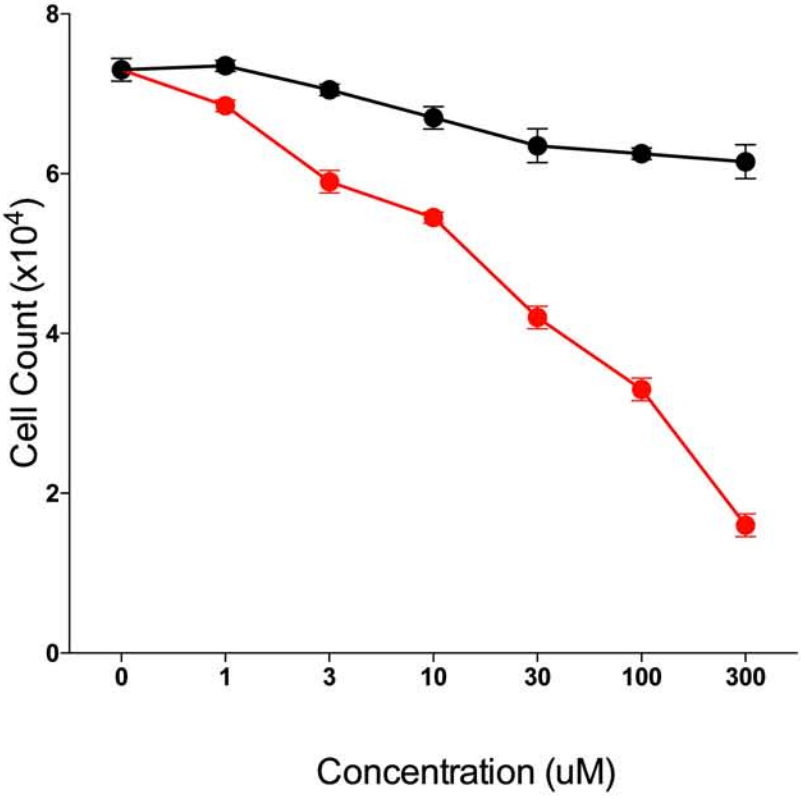
8
6
4
2
0
Cell Count (x10^4)
0
1
3
10
30
100
300
Concentration (uM)

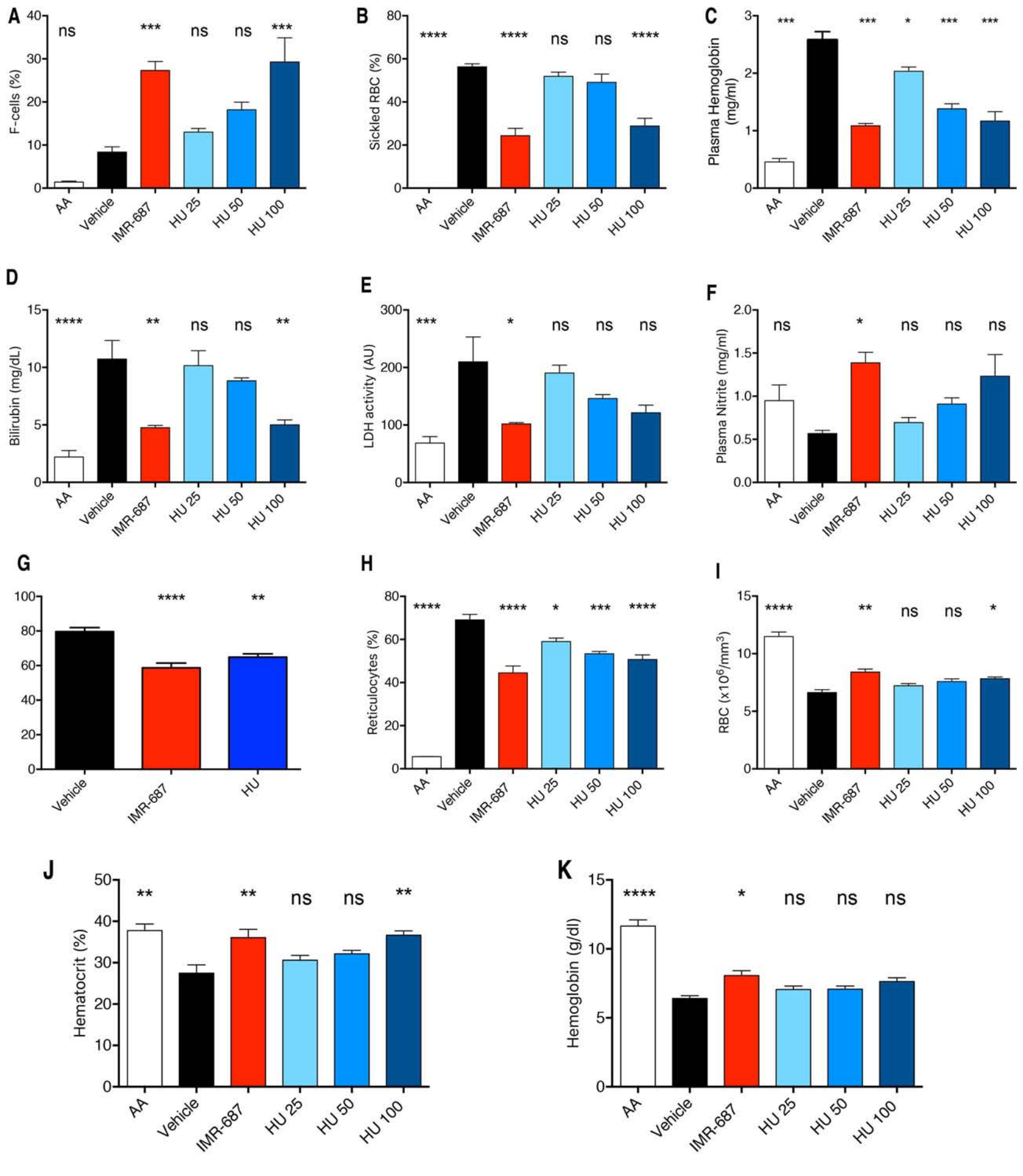
A
F-cells (%)
ns
***
ns
ns
***
AA
Vehicle
IMR-687
HU 25
HU 50
HU 100
B
Sickled RBC (%)
****
****
ns
ns
****
C
Plasma Hemoglobin (mg/ml)
***
***
*
***
***
D
Bilirubin (mg/dL)
****
**
ns
ns
**
E
LDH activity (AU)
***
*
ns
ns
ns
F
Plasma Nitrite (mg/ml)
ns
*
ns
ns
ns
G
****
**
Vehicle
IMR-687
HU
H
Reticulocytes (%)
****
****
*
***
****
I
RBC (x10^6/mm^3)
****
**
ns
ns
*
J
Hematocrit (%)
**
**
ns
ns
**
K
Hemoglobin (g/dl)
****
*
ns
ns
ns

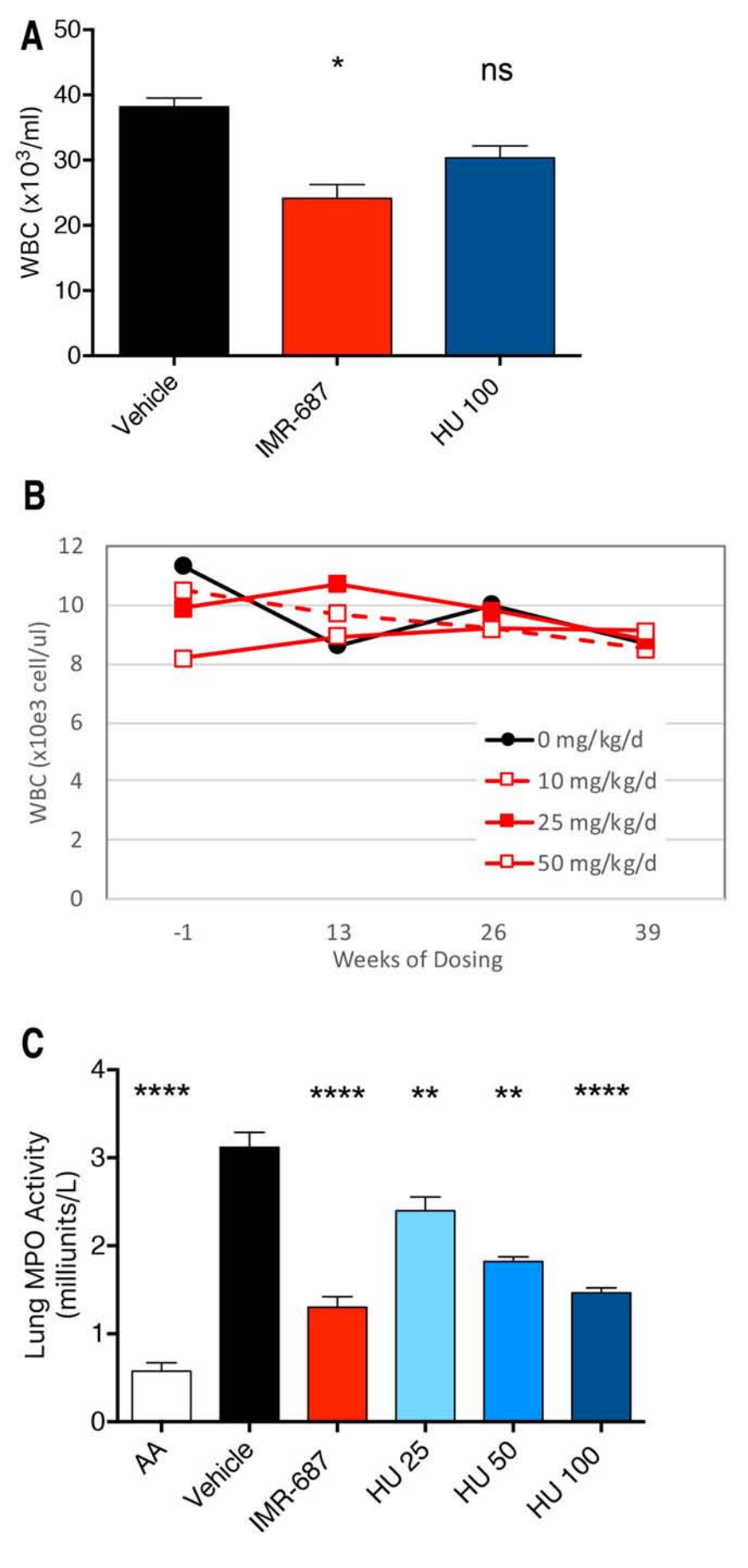
A
WBC (x10^3/ml)
50
40
30
20
10
0
*
ns
Vehicle
IMR-687
HU 100
B
WBC (x10e3 cell/ul)
12
10
8
6
4
2
0
0 mg/kg/d
10 mg/kg/d
25 mg/kg/d
50 mg/kg/d
-1
13
26
39
Weeks of Dosing
C
Lung MPO Activity (milliunits/L)
4
3
2
1
0
****
****
**
**
****
AA
Vehicle
IMR-687
HU 25
HU 50
HU 100

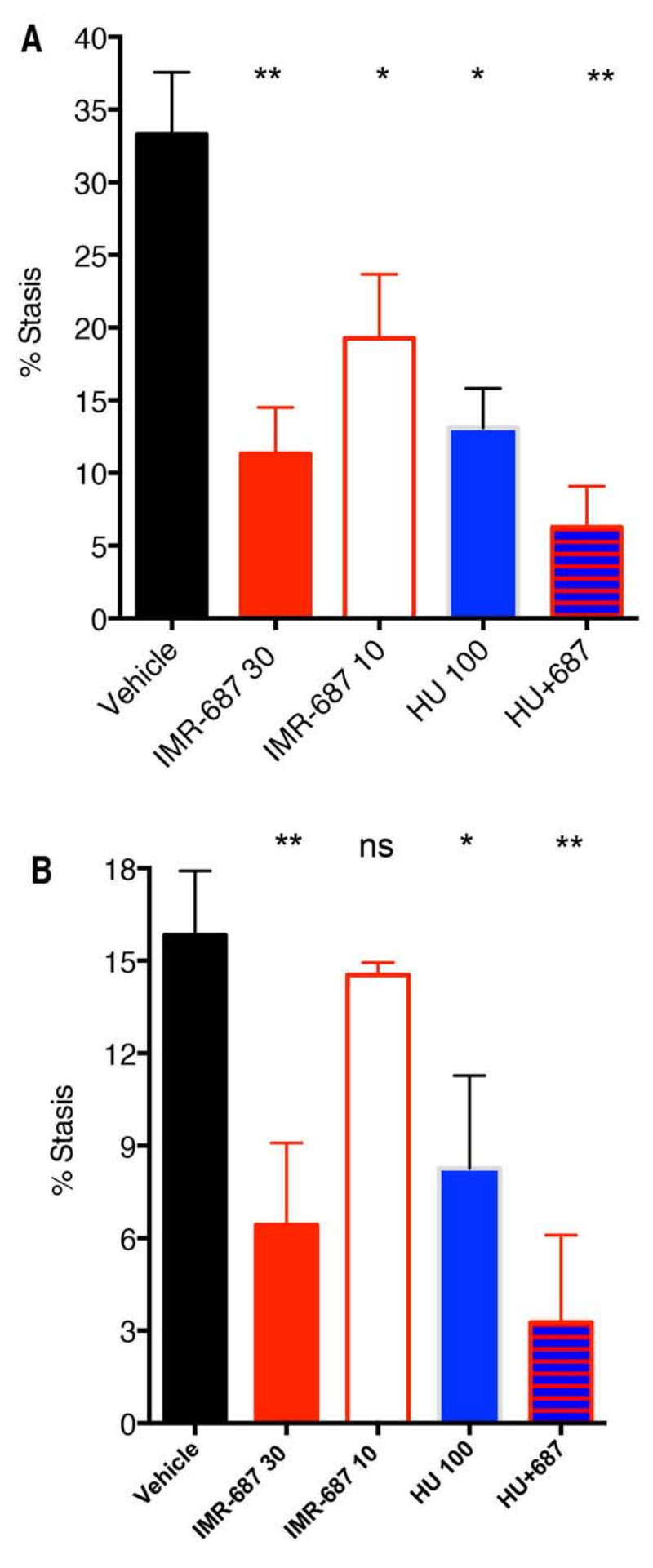
A
40
35
30
25
20
15
10
5
0
% Stasis
**
*
*
**
Vehicle
IMR-687 30
IMR-687 10
HU 100
HU+687
B
18
15
12
9
6
3
0
% Stasis
**
ns
*
**
Vehicle
IMR-687 30
IMR-687 10
HU 100
HU+687

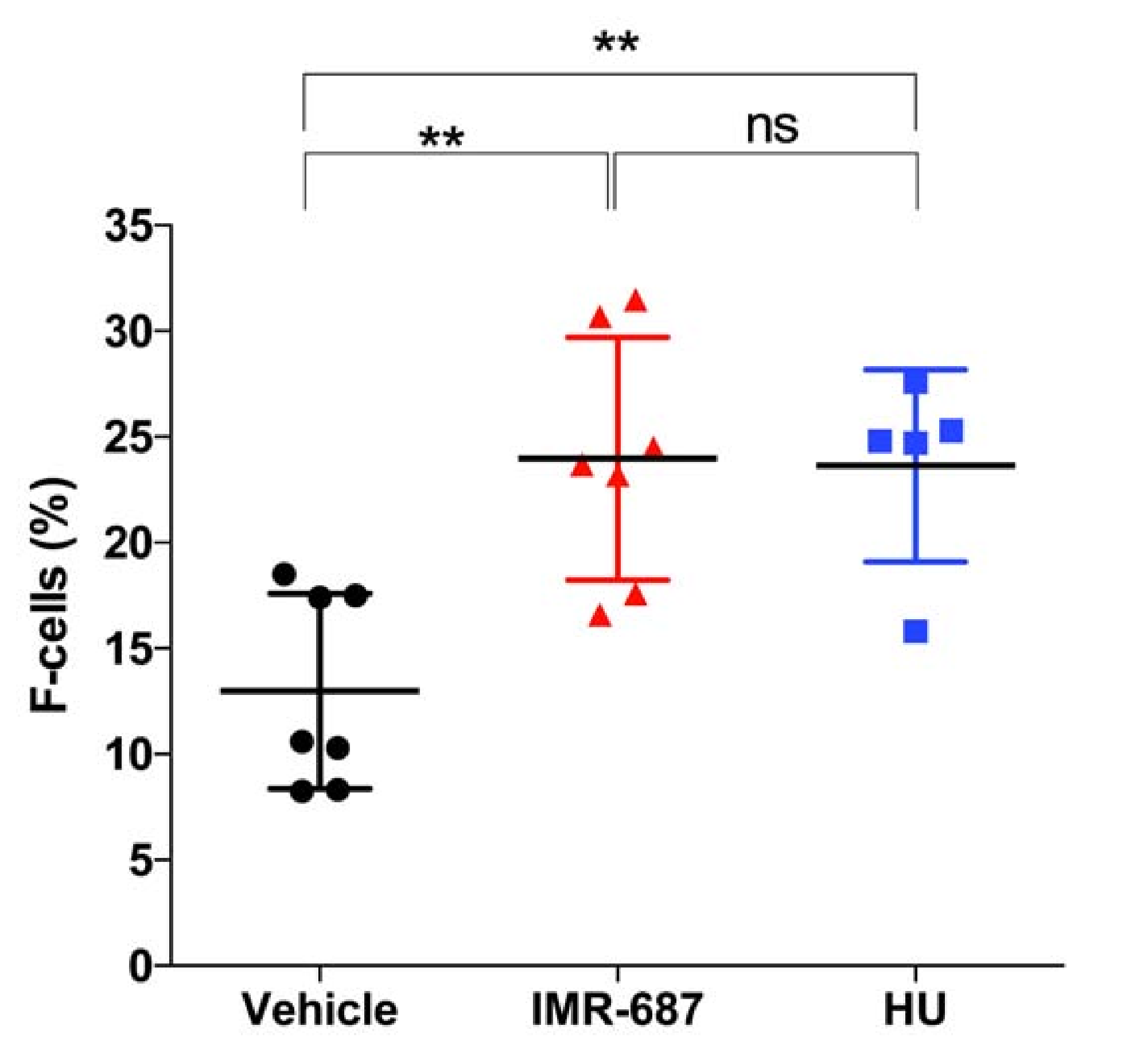
**
**
ns
35
30
25
20
15
10
5
0
F-cells (%)
Vehicle
IMR-687
HU

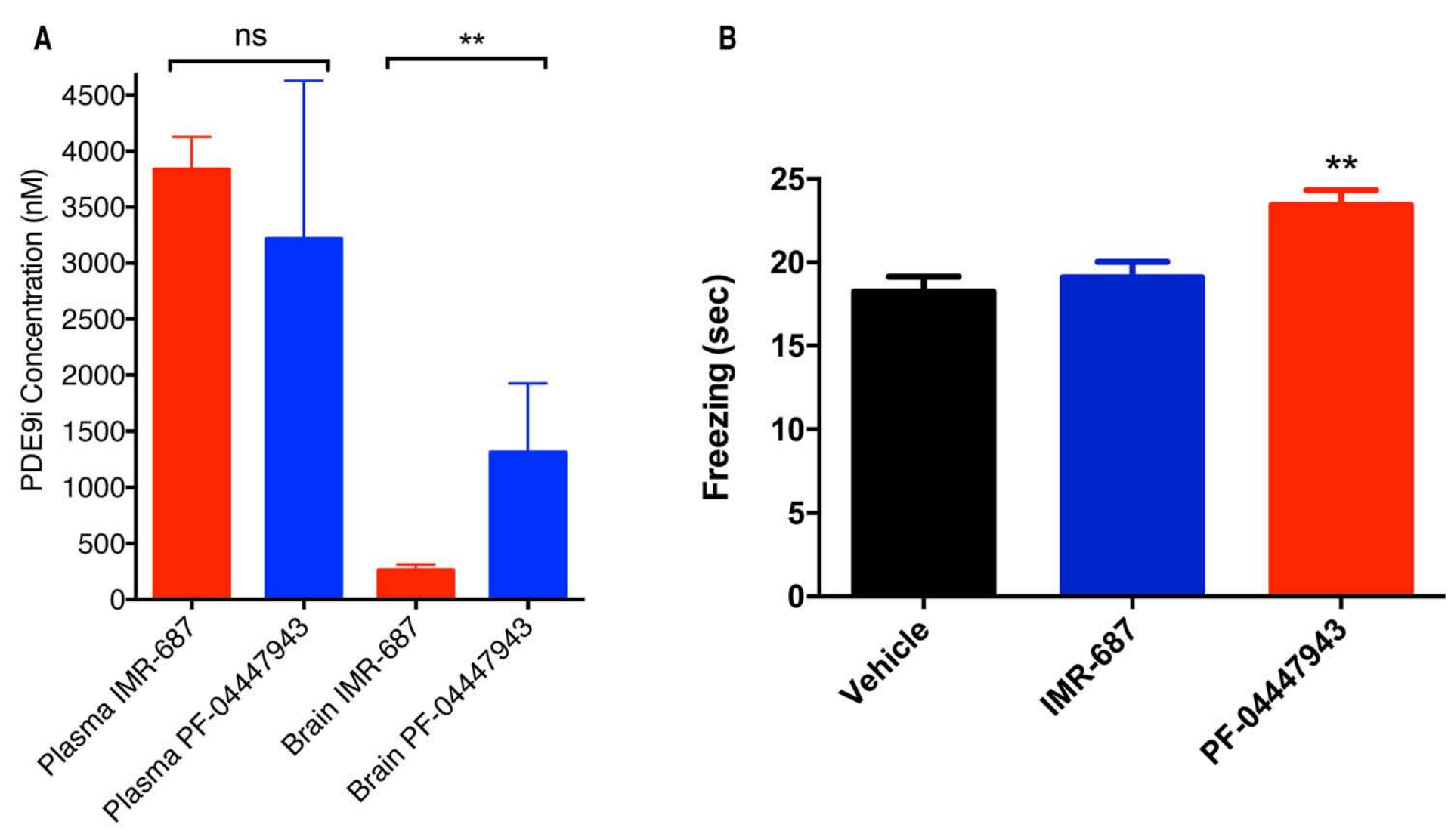
A
ns
**
PDE9i Concentration (nM)
4500
4000
3500
3000
2500
2000
1500
1000
500
0
Plasma IMR-687
Plasma PF-04447943
Brain IMR-687
Brain PF-04447943
B
**
Freezing (sec)
25
20
15
10
5
0
Vehicle
IMR-687
PF-04447943

Supplemental Methods

2.2 K562 and UT-7 erythroid cells

Human erythroleukemic K562 cells (American Type Culture Collection) were cultured in suspension in Iscove's Modified Dulbecco's Medium (ThermoFisher Scientific, France) supplemented with 10% fetal bovine serum, 100 U/ml penicillin, 100 µg/ml streptomycin and 2 mM glutamine (Thermo Fisher Scientific, France). UT-7 cells were cultured in alpha-MEM (with ribo- and deoxyribonucleosides, ThermoFisher Scientific, France) supplemented with 20% fetal bovine serum and 5 ng/ml human GM-CSF (Peprotech, France). Cultures were incubated at 37°C in an atmosphere of 5% CO_2 in air at raised humidity.

2.3 HbF ELISA assay

K562 cells ($5x10^6$) were centrifuged for 5 minutes at 500×g, and the pellet washed three times in cold PBS and suspended in 1 mL ice-cold PBS. Cells were submitted to freeze (-20°C) and thaw cycles (3 times) and centrifuged at 5,000×g for 10 minutes at 4°C to remove cellular debris. Supernatant was assayed using an ELISA kit for HbF (Cloud Clone Corp, CEA996Hu) according to manufacturer instructions. Protein concentration was measured in a 96-well assay plate by a BCA protein assay (Pierce Thermofisher).

2.4 HbF assessment by flow cytometry

Cells were washed in cold PBS, fixed in cold 0.05% glutaraldehyde at RT for 10 minutes, and then permeabilized in 0.1% Triton X-100 at RT for 10 minutes. Cells were then washed with BD Perm/Wash™ buffer (BD Pharmingen) and stained with PE-mouse anti-human HbF at 1/25 (clone 2D12, BD Pharmingen) or isotype control (PE-mouseIgG1κ, clone MOPC-21, BD Pharmingen) for 30 minutes on ice. The percentage of HbF^+ cells (% HbF) and the HbF levels

(MFI) were determined by flow cytometry (GalliosTM, Beckman) in live cells, using FlowJo software (FlowJo LLC, USA).

2.5 SCD patient cells

Blood was collected in a bag containing acid citrate dextrose solution (ACD) from 5 severe adult SCD patients admitted at the Biotherapy Department of Necker Hospital for an exchange transfusion. All samples used in this study were obtained from patients that signed informed consent forms approved by the ethical committee of Necker Hospital on 11 September 2015 (study IMNIS2015-01). Patient ages ranged from 19 to 33 years with a median age of 32 years.

$CD34^+$ cells were isolated from the low density blood cells from a Ficoll density gradient (GE Healthcare Life Sciences) by positive selection using anti-CD34 antibody magnetic cell sorting on Midi-MACS and LS columns (Miltenyi Biotech). Viable cells were suspended in serum-free medium IMDM (Life Technologies) in a 6-well plate (Corning) at a final concentration of $5x10^5$/ml, in the presence of 15% BIT 9500 (mixture of bovine serum albumin [BSA] + insulin + transferrin from Stem Cell Technologies), 100 U/ml penicillin-streptomycin, 2 mM L-glutamine, 10 ng/mL recombinant human (rh) IL-3 (Peprotech), 100 ng/ml rhIL-6 (Peprotech) and 100 ng/ml rhSCF (Peprotech). Cells were incubated for 7 days at 37°C in 5% CO_2 with media replacement on days 3 and 5 and then were pelleted and resuspended in PBS with 2% fetal bovine serum (FBS). $CD36^+$ cells, selected on Mini-MACS and MS columns following incubation with CD36 antibody (Milteny Biotech) and rat anti-mouse IgG1 antibody coupled magnetic microbeads (Miltenyi Biotech), were cultured in media containing 100 ng/mL rhSCF, 10 ng/mL rhIL-3 and 2 UI/ml erythropoetin (Cilag, France). Erythroid differentiation was evaluated by flow cytometry using the following antibodies: FITC-conjugated CD233/Band3 (Miltenyi Biotech,

Germany), APC-conjugated CD49d/α4-integrin (Biolegend – Ozyme, France), VioBlue-conjugated CD235a/GPA (Miltenyi Biotech, Germany) and LIVE/DEAD® Fixable Aqua Dead Cell Stain (Life Technologies, France). Media was supplemented with DMSO, 30 µM HU or 10 µM IMR-687. Cells were split every 2 days with additions of fresh medium. At the end of the 5 days exposure period, the erythroid cells HbF ($LD^-/GPA^+/Band3^+$) was determined by FACS.

2.6 Animals

2.6.1 Townes model

Experiments were approved by the Animal Care Committee at Paris Descartes University. HbSS-Townes mice[42] on a 129/B6 background (Jackson Laboratory, Bar Harbor, ME, USA, 10-12 weeks old with 7/group) were dosed daily by gavage with vehicle (polyethylene glycol in water 1:3), 50 or 25 mg/kg of HU, or 30 mg/kg of IMR-687. On day 30 mice were anesthetized with isoflurane anesthesia, with blood collected from tail vein by heparinized capillaries into EDTA coated tubes and then mice were euthanized and spleens were collected and weighed. Blood counts were measured on a ProCyte Dx Hematology Analyzer (Idexx, France) and reticulocytes were determined using Retic-COUNT Reagent (BD Biosciences Retic-Count Kit). Blood smears were air dried and stained with May-Grünwald-Giemsa and the percentage of sickled RBC was then determined visually by microscopy. Total bilirubin concentrations in plasma were quantified by a bilirubin assay kit (Sigma Aldrich, France). Plasma LDH activity was measured using a LDH assay kit (Pierce – Thermo Scientific, France). Plasma nitrite was determined using Nitrite/Nitrate assay kit (Sigma Aldrich, France). Fetal hemoglobin was assessed by flow cytometry as described above. Total free hemoglobin levels were determined by measuring

absorbance at 540nm (TECAN infinite 200) on 20 µL of plasma mixed with 180 µL of Drabkin's reagent (Sigma Aldrich).

Myeloperoxidase (MPO) and arginase activities were evaluated in lung tissue homogenates. Protein was isolated from lung in RIPA buffer using tissue-ruptor (Qiagen, France). Total protein concentration was determined the by the bicinchoninic acid protein assay (Pierce – Thermo Scientific, France). MPO and arginase activity were detected by using a colorimetric activity assay kit (Sigma Aldrich).

2.6.2 HbSS-Townes vaso-occlusive crisis model

HbSS-Townes mice[42] on a 129/B6 background (6-17 week old with N=3/group) were treated with vehicle (0.08% w/v methyl cellulose), 100 mg/kg of HU, 10 or 30 mg/kg of IMR-687, or 100 mg/kg HU + 30 mg/kg IMR-687 in their drinking water. Experiments were approved by The University of Minnesota's Institutional Animal Care and Use Committee (IACUC). On day 7 of treatment, the mice were implanted with dorsal skin-fold chambers (DSFCs). Three days later, on day 10 of treatment, mice with DSFCs were anesthetized with a mixture of ketamine (106 mg/kg) and xylazine (7.2 mg/kg), placed on a special intravital microscopy stage, and 20-23 flowing subcutaneous venules in the DSFC window were selected and mapped. Mice were then placed in a hypoxic atmosphere chamber (7% O_2/ 93% N_2) for one hour, after which they were returned to room air. All the selected venules were re-examined after one and four hours of re-oxygenation in room air and the number of static (no flow) venules was counted and expressed as percent stasis.

Following completion of the 4h stasis measurement, mice were euthanized via CO_2 asphyxiation, and heparinized blood collected via cardiac puncture, aliquoted and stored at -80°C. Hematocrit was measured using a micro-capillary reader (IEC) after centrifugation in a

micro-capillary centrifuge (IEC). Reticulocytes were measured from blood smears stained with methylene blue. Reticulocytes and total RBC were counted in 4 separate microscopic fields per mouse. Reticulocytes are expressed as a percentage of total RBC. The total white blood cell (WBC) counts were derived manually using a hemocytometer.

To measure irregular shaped RBC, heparinized whole blood from HbSS- and HbAA (control)-Townes mice was incubated for 15 minutes at 4^{o}C with an equal volume of 2% sodium metabisulfite and fixed post-incubation with an equal volume of 10% neutral buffered formalin. Fixed blood smears (10 µL) were prepared on glass slides and 3 representative fields were photographed at 100X magnification. Irregular and normal shaped RBC were counted (mean = 99 ± 15 cells/slide) and the irregular shaped RBC were expressed as a percentage of total RBC. The irregular shaped RBC included teardrop, schistocyte, elliptocyte, bite and sickle cells.[43]

HbF+ cells were stained on blood smears by the Kleihauer-Betke method using a fetal cell stain kit (Simmler).[44] HbF+ cells and total RBC were counted in four separate microscopic fields at 100 X magnification per mouse. Plasma hemoglobin and bilirubin were measured spectrophotometrically by the Fairbanks AII method.[45] Total plasma heme levels were measured colorimetrically at 400 nm using a QuantiChrom^{TM} heme assay kit (BioAssay Systems).

2.7 Fear Conditioning Model

Test articles or vehicle were administered (PO) 30 minutes prior to training and testing.

Training, Day 1, mice were placed into a 7”x7”x12” CFCC enclosure with an electrified grid bottom. After a 120s period of exploration and habituation, they received three tonal cue (30s, 3kHz, 75dB) and mild foot shock (1.5s, 0.65mA) pairings separated by 30 second Inter-Trial-Interval (ITI) rest periods. They were then allowed to remain in the same enclosure for a final

post-shock interval (FPSI, 30s). Animals were then removed from the CCFC enclosure and returned to their home cages.

Contextual testing, Day 2, mice were exposed to the CFCC enclosure for 300 seconds with no tones played and no shocks emitted. Freezing behavior was measured and used as an endpoint for memory over a period of time similar to the original exploration and habituation time. Mice were then returned to their home cage.

Cued testing, Day 2, after contextual session, mice were again placed into the CCFC chamber with a novel context (black insert). After a 300s period of exploration and habituation, they received five CS tonal cues (30 s, 3 kHz, 75 dB) separated by 60s ITIs. Thirty second tones were played at 300s, 390s, 480s, 570s, 660s and the session ended after the final ITI. Mice were then returned to their home cage.

Time spent freezing during the training, contextual, and cued phases of the evaluation were scored automatically via the MedAssociates Software.

2.8 Statistical analyses

Statistical analyses studies were performed using a one-way analysis of variance (ANOVA) test followed by a Dunnett's test (multiple comparison test) or Kruskal-Wallis test (non-parametric) for analysis of treatment effect versus controls. All statistical analyses were derived using GraphPad software (v6.00, San Diego, California, USA). Statistical significance to reject the null hypothesis was identified at the $p<0.05$ level. For illustrative purposes, significance levels of $p<0.01$ and $p<0.001$ were also noted.